

CFD and Experimental Simulation of the Laminar-Turbulent Transition on the HEXAFLY-INT Glider Model

Voevodenko Nina*, Gubanov Anatoly*, Ivanyushkin Dmitry*, Shvaley Yury* and Steelant Johan**

* Central Aerohydrodynamic Institute named after Professor N.E. Zhukovsky (TsAGI)

1 Zhukovsky Street, Zhukovsky Moscow Region, 140180 Russian Federation

** European Space Agency – European Space Research and Technology Center (ESA-ESTEC)

The Netherlands

Abstract

At high supersonic flight speeds the laminar-to-turbulent transition (LTT) is one of most important physical phenomenon which influence on the vehicle aerodynamics. Therefore, in the framework of the international project HEXAFLY-INT the studies are conducted to determine the LTT on the surface of the EFTV glider model. This paper presents the results of CFD simulation of the flow with LTT on the EFTV surface, as well as experimental studies of the flow with LTT around EFTV model in the wind tunnel. Also CFD and experimental results are compared with the assessment based on empirical correlations obtained on flat plates and cones.

1. Introduction

The phenomenon of the laminar-to-turbulent transition in the boundary layer on the aircraft surface has a significant influence on the aircraft aerodynamic characteristics at high supersonic flight speeds. LTT affects substantially on the thermal processes, on the drag coefficient and on the vehicle Lift-to-Drag ratio. Therefore, in the framework of the international project HEXAFLY-INT intended to build the high-speed passenger aircraft, the studies are conducted to determine the LTT on the surface of the HEXAFLY-INT glider model - EFTV (Experimental Flight Test Vehicle). This paper presents the results of numerical simulation of the flow with LTT on the EFTV surface, as well as experimental studies of the flow with LTT around EFTV model in the wind tunnel. In addition, the results of numerical simulation and experiment are compared with the results obtained from empirical formulas for the position of the onset of the LT transition and its extent on the surface of a flat plate and cone.

The geometry of the HEXAFLY-INT - EFTV Glider studied in this project is shown in Figure 1. The EFTV is a hypersonic glider of 3.29m length with a span of about 1.23m. It has a two-dimensional nose with leading and lateral edges of 2mm radius. The wing has a 80° sweep angle, a 14° negative dihedral angle, and a leading edge of 1mm radius. The vehicle is equipped by a couple of active ailerons (0.4m long and 0.32m wide) deflectable in a symmetric and asymmetric way to control the flight, and a couple of fixed vertical fins with 68.5° sweep angle and a 54° angle formed between the two fins in the transversal plane.

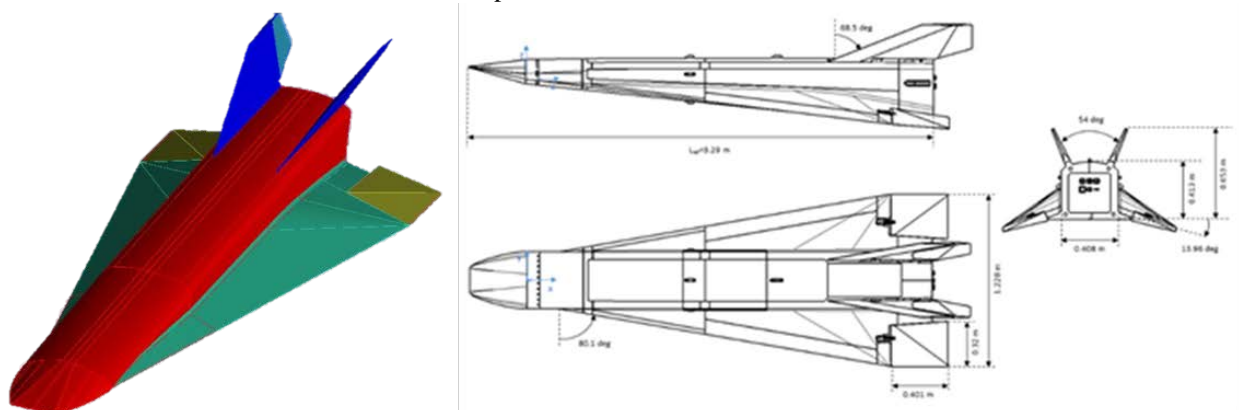


Figure 1: Геометрия the Experimental Flight Test Vehicle (EFTV) HEXAFLY-INT.

The EFTV geometry and scientific mission profile have been developed on the basis of the previous European projects HEXAFLY [1], LAPCAT I & II, ATLLAS I & II and use a preliminary high-speed vehicle concept and related technologies. A waverider configuration was chosen to demonstrate a hypersonic gliding cruise within the atmosphere.

The main preliminary flight sequence profile and flight events are shown in Figure 2. The EFTV will be lifted to the suborbital trajectory with apogee at about 90 km by a sounding rocket, i.e. the Brazilian VS43 launcher equipped by an 8 ton solid rocket motor (trajectory segment 1 – 5). After the release from the launcher, the EFTV will perform the descent first part (trajectory segment 6 - 7) docked to the Experimental Support Module (ESM), which controls the vehicle attitude by means of a cold gas system (CGS). As soon as the EFTV enters to the phase of full aerodynamic control, it separates from the ESM and stops its descent to perform a hypersonic cruise at approximately Mach 7 (trajectory segment 8 - 10). In this experimental phase, the EFTV aims to demonstrate a high aerodynamic efficiency ($L/D \geq 4$), a positive aerodynamic balance ($L \geq W$) at controlled cruise Mach number of 7, an optimal use of advanced high-temperature materials and structures. Further details can be found in [2][3].

Numerical and experimental simulations of flow around EFTV were performed for the values of the basic parameters corresponding to the conditions of the flight experiment planned in the HEXAFLY-INT project, namely $M_\infty = 7, 7.5$, $\alpha = -5^\circ, 0, 3.6^\circ, 15^\circ$, $Re = 12 \times 10^6$ for $M_\infty = 7$ and $Re = 3.63 \times 10^6$ for $M_\infty = 7.5$ at zero angle of slip and symmetrically deflected ailerons on the angle $\delta = -15^\circ$. These regimes correspond to the trajectory segment 8-9-10 on Figure 2.

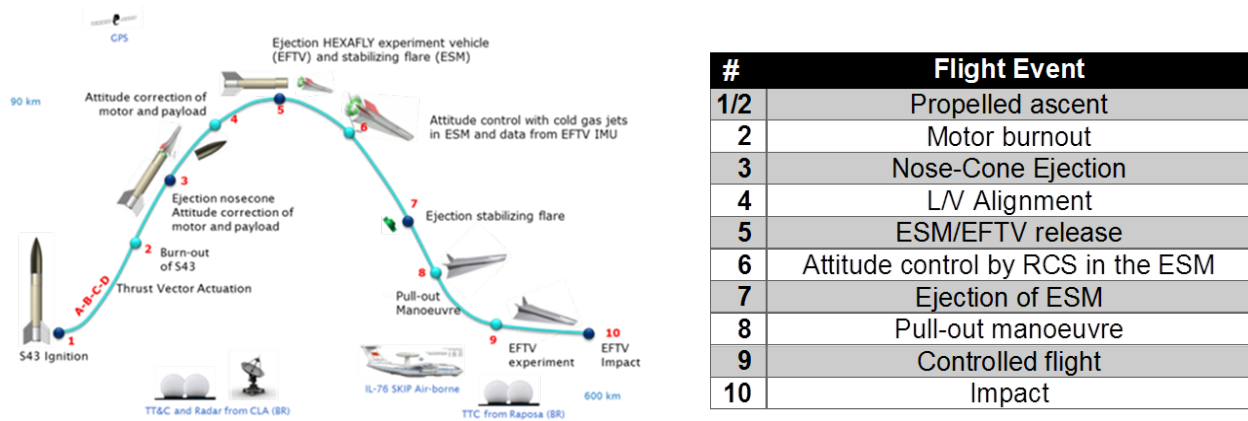


Figure 2: Flight sequence profile.

For the numerical simulation of the flow field around the EFTV model ANSYS FLUENT software package was used. Numerical simulations were performed on the basis of the Reynolds Averaged Navier - Stokes (RANS) solutions. To simulate the flow with the LT transition in the boundary layer, two different models of turbulence were used, in which the position of the LT transition is determined automatically, and a comparison of their results is made. Mainly to simulate the flow with LTT it was used the turbulence model “Langtry & Menter SST-Transition Model”, in which LTT position is determined automatically based on LCTM concept (Local Correlation-based Transition Modelling). Second model was the k-kl- ω model with a laminar-turbulent transition (Walters & Leylek k-kl- ω Transition Model). The default settings of this model defined in FLUENT package have been used in computations.

The EFTV HEXAFLY-INT glider model of scale of 1: 3 was manufactured by TsAGI, and it was tested in the hypersonic wind tunnel of TsAGI T-116. The LTT region on the model surface was determined by the method of the thermal heat transfer coefficient values (the number of Stanton), which was determined with the help of special thermal sensors. Determination of the transition region is based on a significant difference in the Stanton numbers in laminar and turbulent boundary layers.

In this paper, we present the results of the numerical simulation of the LT transition on the EFTV surface, as well as the experimental studies of the LT transition on the EFTV model in a wind tunnel. In addition, the results of numerical simulation and experiment are compared with the results obtained by ESA from empirical formulas for the position of the onset of the LT transition and its extent on the surface of a flat plate and cone.

2. CFD simulation

Numerical simulation of laminar-turbulent transition is a very difficult task even for the modern level of development of computer technology and numerical methods. A correct numerical simulation of LTT is possible only on the basis of direct numerical simulation of the Navier-Stokes equations solution (DNS methods). However, even supercomputers now allow simulating the three-dimensional non-stationary DNS solutions only for fairly simple geometries, such as a plate or cone. Building a DNS solution for such a complex geometry as the EFTV HEXAFLY-INT surface is technically impossible because it requires computational volumes and computer resources that do not exist in principle. Therefore, numerical studies were carried out within the framework of the Reynolds averaged Navier-Stokes (RANS) equations. This approach is not completely correct, but it allows, at least, to obtain approximate results, which, of course, require verification and comparison with the experimental data.

The studies were carried out for the flight conditions of the EFTV glider under conditions of continuous medium, with air being considered as an ideal gas. Even in the case of CFD simulation of hypersonic flows, the assumption of an ideal gas remains valid, since the aerodynamic shape of EFTV is a thin body with small angles of inclination of the surface to the incoming stream (the front edge radius is 2 mm) and the flight will pass at small angles of attack. To calculate the flow field around the EFTV model, the ANSYS FLUENT software package was used. Numerical simulation was performed on the basis of the RANS equations solution. The condition for equilibrium radiation with a radiation coefficient $\epsilon = 0.4$ was specified on the walls. For calculations, an unstructured grid of 20,000,000 cells per half-model was used. In the boundary layer, on average, there were 35 cells in thickness. The investigations were carried out for the full-scale model $L = 3.29$ m. An example of a computational grid is shown in Figure 3.

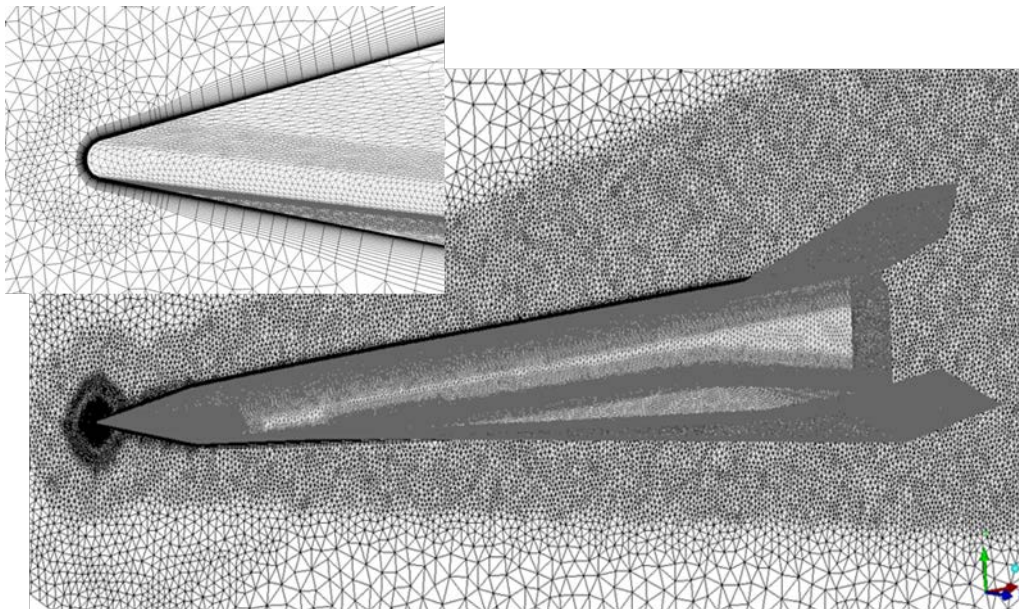


Figure 3: Computational grid.

Two different methods of the laminar-to-turbulent transition modeling were used in this work, namely:

- Tran1 (main): SST $k-\omega$ turbulence model supplemented by the laminar-turbulent transition model Langtry - Menter (in the descriptions of the FLUENT package called Langtry & Menter SST-Transition Model), in which the position of the LT transition is determined automatically based on the LCTM concept (Local Correlation- Based Transition Modeling);
- Tran2 (additional): $k-k_l-\omega$ model with a laminar-turbulent transition (in the descriptions of the FLUENT package is called Walters & Leylek model with additional equation for the laminar flow kinetic energy).

The calculations used the standard settings of the turbulence model data specified in the ANSYS FLUENT package. It should be noted that these models were created and is typically used for simulation of flows at subsonic speeds, so the decision to use theirs for the simulation of flows at hypersonic speeds is a bold and requires validation and a critical approach to the results based on a comparison with experimental data.

Figure 4 shows an example of the results of the LT transition simulation on the surface of the EFTV model with $M_\infty = 7$, AoA $\alpha = 0^\circ$, and the angle of the ailerons deviation $\delta = 15^\circ$. Flow patterns with LT transition were obtained using the Tran1 model. The left picture shows the flow on the EFTV leeward side, and the right picture shows the

flow on the EFTV windward side. The region of the laminar-turbulent transition was determined by value of the turbulence intensity parameter

$$Tu = \frac{\sqrt{\frac{2}{3}k_\delta}}{U_\delta} \times 100\% ,$$

where k_δ is the kinetic energy of turbulence, and U_δ is the velocity. It was assumed that the loss of stability of the laminar flow and the onset of the transition to turbulent flow occurs at $Tu \geq 0.5\%$.

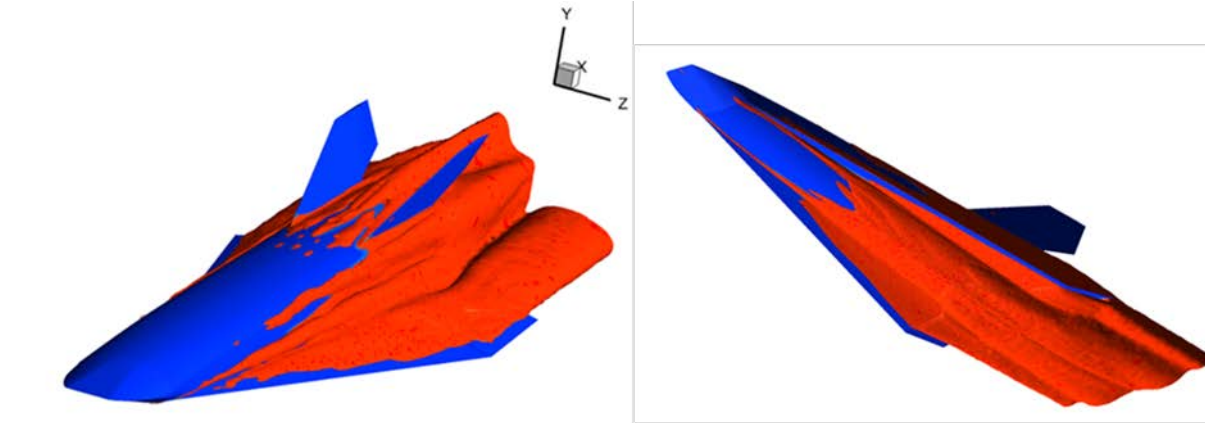


Figure 4: Transitional flow areas on leeward (left) and windward (right) sides obtained by the criterion of $Tu > 0.5\%$; $M_\infty = 7$, $\alpha = 0^\circ$.

All grid cells, where $Tu \geq 0.5\%$, are colored in red, those cells where $Tu < 0.5\%$ are colored in blue. Referring to Figure 4, the transition in the symmetry plane on the windward side of the model occurs at the distance of ≈ 1.3 m from the leading edge, and on the leeward side - at the distance of ≈ 1.8 m.

The turbulence intensity Tu distribution in the boundary layer at the distance ≈ 2 mm from the surface of the model is shown in Figure 5. It was assumed that the flow is completely turbulent at $Tu \geq 1\%$, that is, the transition zone is colored from green to red. As seen in Figure 5, on smooth surfaces (fuselage, wing), where the flow is relatively homogeneous, the LT transition occurs in a relatively narrow region, and the transition line is seen quite clearly. However, in regions of complex vortex flows, for example, in the fuselage-wing fusion region, the transition region is strongly smeared and covers a significant part of the model surface. The distribution of the intermittency parameter γ in the flow field around the EFTV model, shown in Figure 6, confirms the conclusions drawn.

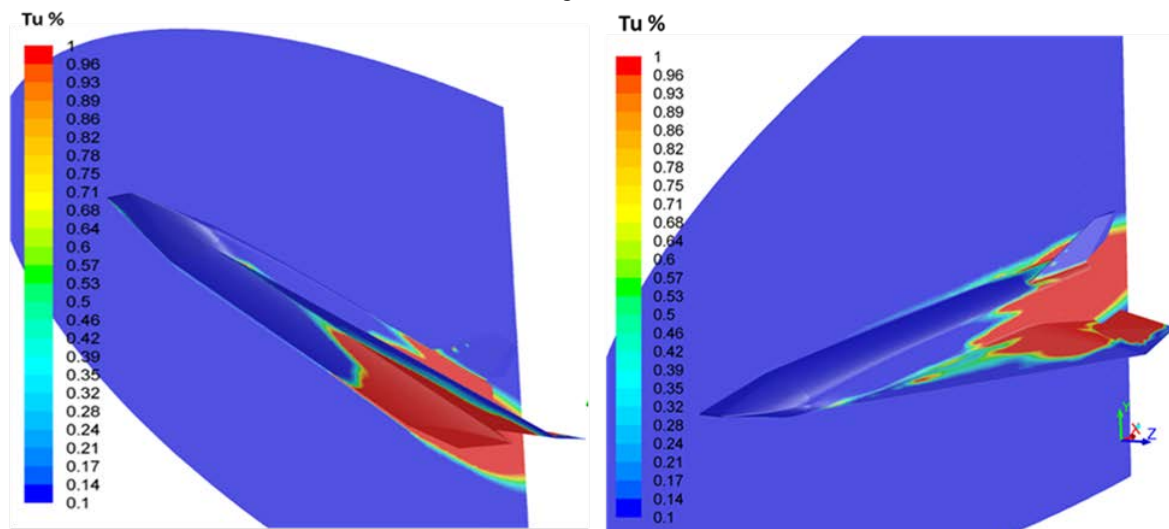


Figure 5: The Tu distribution in BL on distance ≈ 2 mm on the leeward side (right picture) and on the windward side (left picture) of HEXAFly-INT model; $M_\infty = 7$, $\alpha = 0^\circ$.

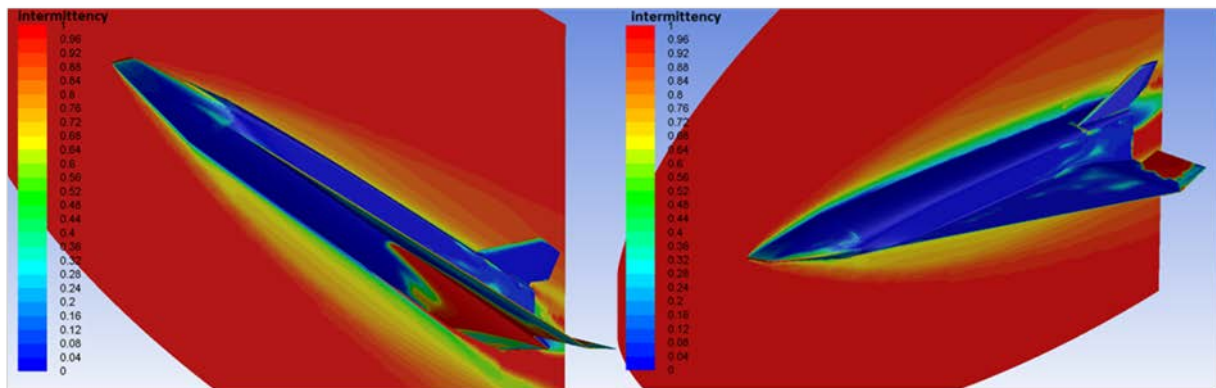


Figure 6: The intermittency distribution on the leeward side (right picture) and on the windward side (left picture) of HEXAFLY-INT model; $M_\infty=7$, $\alpha=0^\circ$.

Figure 7 shows the field of Mach number around EFTV at $M_\infty = 7$ and $\alpha = 0^\circ$. Black lines show lines of constancy (isolines) of the Mach number. They allow us to visualize the vortex pattern of airflow around the aircraft. As it is visualized on Figure 7, the vortices are generated by the EFTV nose and propagate downstream. These vortices become more intense as the angle of attack increases and lead to the development of big transitional zones on the surface elements where they come, i.e. in the fuselage-wing fusion regions (see Figure 5, right picture).

Figures 8 - 9 show the results of numerical simulation of the flow and LTP fields with the Tran1 model at $M_\infty = 7$ and the increasing angle of attack $\alpha = 3.6^\circ$, 5° and 15° . Figure 8 shows the flow turbulence regions in the inner volume of the calculated region, obtained by the criterion: the flow is turbulent, if $Tu \geq 0.5$, and also the Mach number fields with isolines is shown by Figure 9.

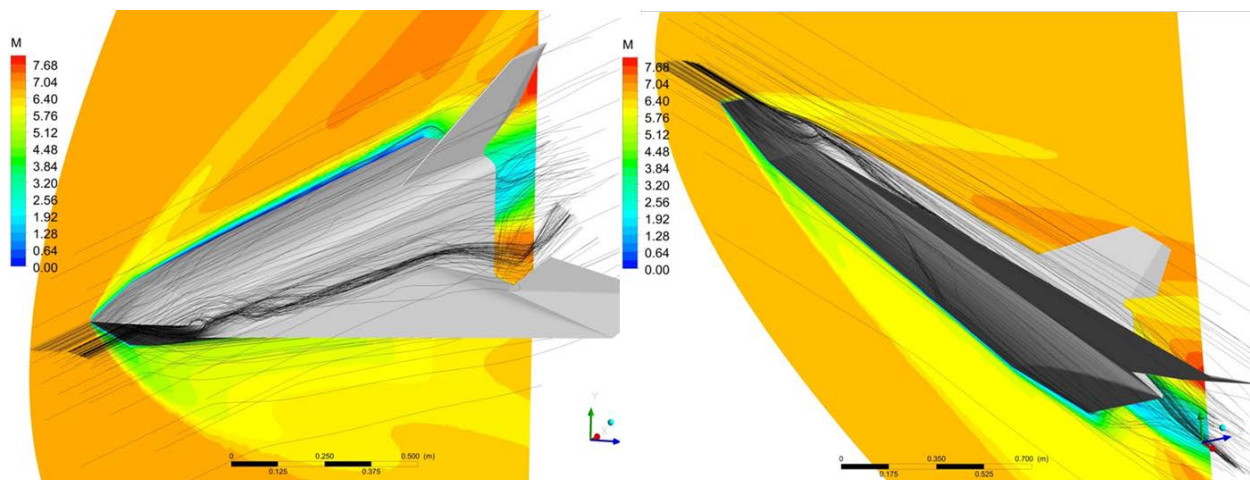


Figure 7: LTT simulation (Tran1) at $M_\infty=7$ and $\alpha=0^\circ$ - Mach number flow fields on the leeward side (right picture) and on the windward side (left picture) of HEXAFLY-INT model.

The flow patterns presented in Figures 8-9 show the following characteristic features:

1. In most cases, the current, both on the windward and leeward surfaces of the aircraft under study, is transitional.
2. The LTT region as the transition line on the aircraft surface has a complex shape.
3. On the windward surface of the aircraft the LTT takes place at all angles of attack. The transition area is located in the around middle part of the windward surface.
4. On the leeward surface of the aircraft the transition region is displaced downstream with an increase of the angle of attack, and at $\alpha = 15^\circ$ the flow on the leeward surface becomes completely laminar.
5. The vortices are generated by the EFTV nose that propagate downstream. These vortices become more intense as the angle of attack increases. When hit on surface elements located downstream, such vortices can lead to significant changes in the aerodynamic characteristics of these elements.

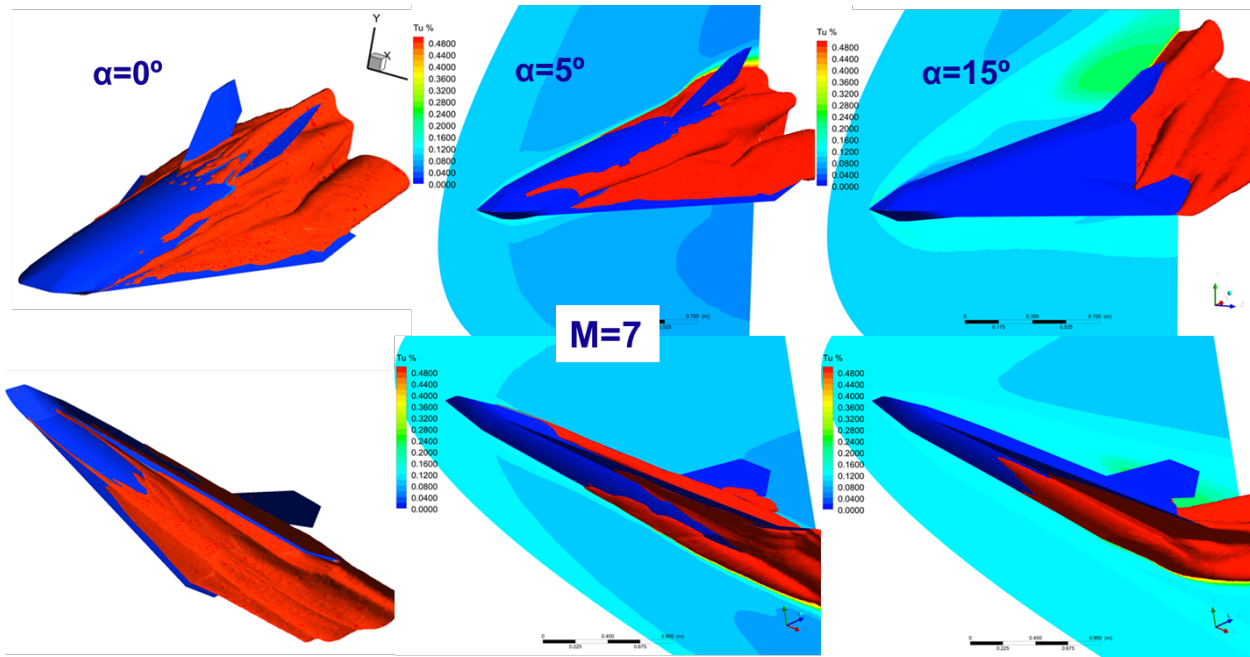


Figure 8: LTT simulation (Tran1) at $M_\infty=7$ и $\alpha=0^\circ, 5^\circ, 15^\circ$ - LTT regions obtained by the criterion of $Tu>0.5$.

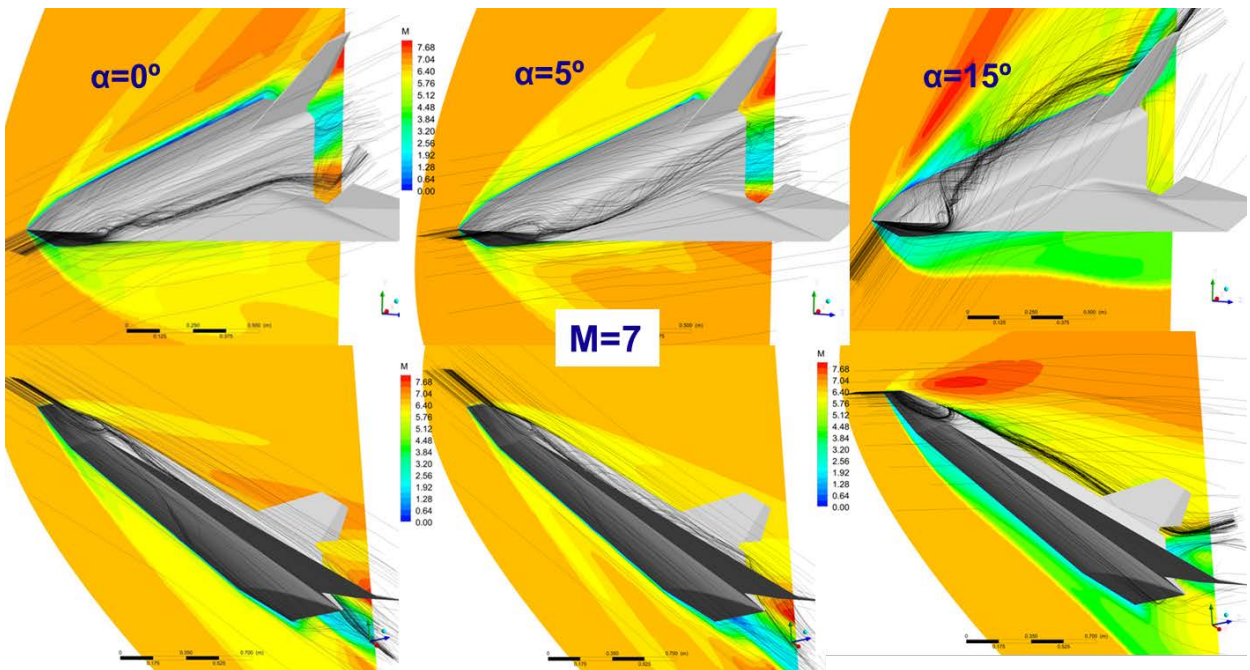


Figure 9: LTT simulation (Tran1) at $M_\infty=7$ и $\alpha=0^\circ, 5^\circ, 15^\circ$ - Mach number flow fields on the leeward side (upper pictures) and on the windward side (bottom pictures) of HEXAFLY-INT model.

Also in the frame of this project, the calculations with three different turbulence models: SA, TM1 and TM2, are performed previously for a fully turbulent boundary layer (BL), and the results were compared with results of simulations with Tran1 and Tran2 LTT models. A comparison of the resulting lift coefficient C_L , the drag coefficient C_D and longitudinal moment coefficient M_Z is shown in Figure 10. The lift coefficients obtained in the simulation with different turbulence models and LTT models are very close in the whole range of investigation. However, the values of the drag coefficient and the longitudinal moment coefficient M_Z obtained by different simulations are very different. A significantly higher C_D value is given by the simulation with completely turbulent boundary layer with the $k-\epsilon$ and the SA turbulence models. Both models with LTT give close results with the $k-\omega$ model SST.

A significant difference in the value of the aerodynamic drag coefficient when modeling the state of the boundary layer by different methods (laminar BL, turbulent BL with different turbulence models and BL with LT transition) leads to a noticeable difference in lift-to-drag ratio. Depending on the method of the BL modeling the maximum lift-to-drag ratio can vary from 4. to 6. Thus, different turbulence models and LTT models give different results on the total characteristics, and further validation of the numerical methods is necessary to obtain reliable results.

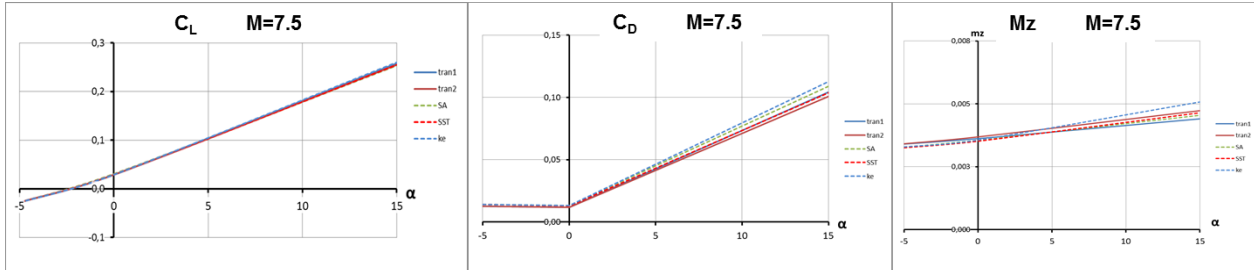


Figure 10: Comparison of aerodynamic coefficients obtained in numerical simulation with different turbulence models and LTT models.

A comparison of the flow patterns around EFTV obtained in simulation with two different LTT models Tran1 and Tran2 is presented in Figure 11. It is interesting to note that the Mach number fields obtained with Tran1 and Tran2 practically coincide, while the fields Tu - parameter showing LTT are significantly different.

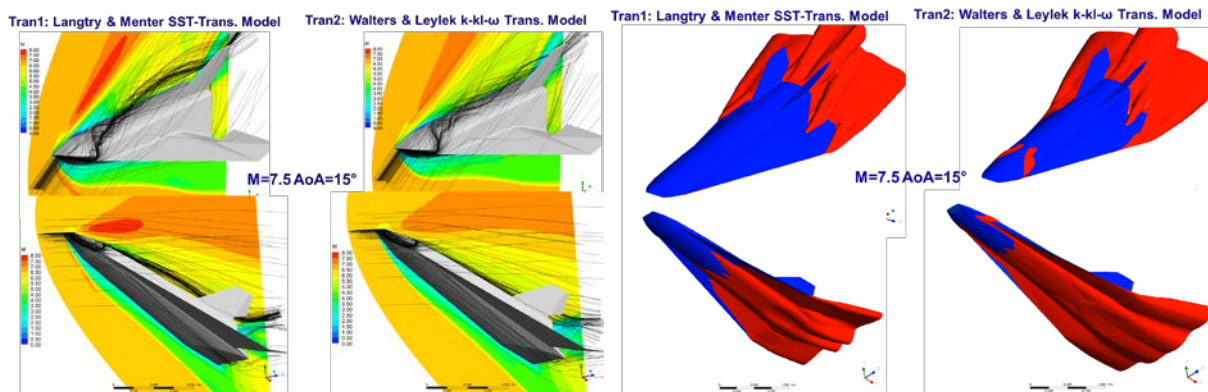


Figure 11: Comparison of Mach number fields (left) and Tu fields (right) obtained in numerical simulation with LTT models Tran1 and Tran2.

The CFD studies have shown a significant influence of the physical picture of the flow in the boundary layer on the vehicle drag coefficient and on its lift-to-drag ratio. Therefore, the task of these studies was to determine the effect of the boundary-layer state and the choice of the turbulence model on the aerodynamic characteristics of the aircraft and its elements. However, data obtained by CFD methods require verification and validation. Therefore, along with the CFD studies, a series of tests were performed in the TsAGI's wind tunnel T-116, aimed at determining the laminar-turbulent transition pattern on the surface of the EFTV HEXAFLY-INT model.

3. Experimental Wind Tunnel Campaign

Experimental studies of the EFTV HEXAFLY-INT model were conducted in TsAGI's wind tunnel T-116. The EFTV model installed in the T-116 test section is shown on Figure 12.

The T-116 wind tunnel (WT) have the squared test section of 2.35m×1m×1m size and allows to carry out a wide variety of aerodynamic research of the aircraft models and of their components at super- and hypersonic flow velocities. The Mach number in the WT tests section varies from M=1.8 up to M=10. The unit Reynolds number Re variation range (referred to model length of 1m) is from 2.5·10⁶ up to 42·10⁶. These data correspond to modeled full-scale Re-numbers for 15 – 40 km height for flying vehicles (for characteristic vehicle length L=6 m). The T-116 Test Facility is a blow-down WT of ejector type with exhaust into atmosphere, with a variable supersonic diffuser and

three-staged ejector. The tunnel is powered by pressure tank; the air is exhausted into atmosphere. The WT is equipped with electric heaters in order to prevent the air condensation in the test section.

T-116 is a unique facility, it is super- and hypersonic WT of continuously working regime (test duration up to 7 minutes). It makes possible to obtain the steady-state flow pattern, and so, the results obtained correspond to the flight conditions more adequately, than those obtained in short-run WTs. This enables more proper link between wind tunnel and flight experiments and improves the understanding of the relevant flow physics and to further validate and improve the applied CFD tools.

TsAGI produced the windtunnel model of a scale of 0.35 with respect to the size of the real EFTV vehicle. The windtunnel model and a general view of the wind tunnel are presented in Figure 12. The tests were conducted at Mach number $M = 7$ and angles-of-attack of the model $AoA = 0, 2^\circ, 3.6^\circ,$ and 12° . The flow parameters realized in the working chamber of T-116 during tests are shown in Table 1.



Figure 12: EFTV wind tunnel model and T-116 wind tunnel at TsAGI

Table 1: This is a table example

M	P_{tot} , atm	T_{tot} , K	$Re_{1M} * 10^{-6}$	Simulated flight altitude H, km
6.99	22	675	7.66	30

Laminar-to-turbulent boundary layer transition on the model surface was investigated using the so called ‘regular heating regime method’. The method is based on significant difference between the local heat transfer coefficients on the model surface corresponding to laminar and turbulent boundary layers. Local heat transfer coefficients are determined measuring the rate of temperature change on specially prepared elements of the model surface during the wind-tunnel tests. The method was developed by G.M. Kondratiev [5] and further modifications were elaborated in several subsequent scientific works.

The local flow parameters outside of the boundary layer on the wind- and leeside of the model used for calculations of local heat transfer coefficients, were determined approximately using relations for the oblique shock-waves and Prandtl–Meyer expansion flows, using the local angles of inclination of the model surface to the free-stream flow. The values determined in this way are given in Table 2. These parameters are used to determine local equilibrium temperatures for laminar and turbulent boundary layers, and also corresponding Stanton and Reynolds numbers:

$$T_{r,lam} = T_{\delta}(1+0,168M_{\delta}^2) \quad T_{r,turb} = T_{\delta}(1+0,178M_{\delta}^2) \quad (1)$$

$$St_{\delta} = \frac{\alpha_{\delta}}{\rho_{\delta}v_{\delta}c_{\delta}}, \quad Re_{\delta} = \frac{\rho_{\delta}v_{\delta}}{\mu_{\delta}} \times \rho_{\delta}v_{\delta} = 0.0697 \frac{P_{\delta}M_{\delta}}{\sqrt{T_{\delta}}}$$

Where P_{δ} , M_{δ} and T_{δ} are the local flow parameters outside of the boundary layer. Stanton numbers obtained from the experiment are compared with their reference values corresponding to laminar and turbulent boundary layers, i.e. for laminar boundary layer [6]:

$$St_{\delta,lam} = 0,415 Re_{\delta}^{-0.5} (1+0.168M_{\delta}^2)^{-0.116} (T_w/T_r)^{-0.116} \quad (2)$$

and for turbulent boundary layer [7]:

$$St_{\delta,turb} = 0,028 Re_{\delta}^{-0.18} (1+0.178M_{\delta}^2)^{-0.47} (T_w/T_r)^{-0.24} \quad (3)$$

Table 2: The local flow parameters used for calculations of local heat transfer coefficients.

AoA	Location	P_{δ} [N/m ²]	T_{δ} [K]	M_{δ} [-]	$\rho_{\delta}v_{\delta}$ [kg/m ² /sec]	$T_{r,lam}$ [K]	$T_{r,tur}$ [K]
$\alpha=0$	Wind-side	1360	84.4	5.92	61.05	581.3	610.9
	Leeside	525	62.7	6.99	32.3	577.4	608.0
$\alpha=2^{\circ}$	Wind-side	1801	94.4	5.56	71.7	584.7	613.8
	Leeside	360	56.3	7.41	24.8	575.6	606.6
$\alpha=3.6^{\circ}$	Wind-side	2206	102.5	5.29	80.4	584.3	613.1
	Leeside	279	52.4	7.72	20.8	577.1	608.3
$\alpha=12^{\circ}$	Wind-side	5678	173.1	3.81	114.6	595.2	620.4
	Leeside	46	31.3	10.22	5.88	580.9	613.2

Empirical formulas (1), (2) and (3) are obtained on the basis of the experience obtained during many years of tests in the TsAGI's wind tunnel T-116 and generalized in [6] and [7]. These formulas are used in TsAGI to determine LTT. Similar empirical formulas are used in their studies by specialists from ESA and CIRA. A detailed description of the empirical methods used by ESA and CIRA in LTT studies is given in [8].

In experimental studies, the local values of the heat transfer coefficient are determined by measuring the rate of change in surface temperature by means of special thermocouples whose location on the surface of the model is shown in Figure 13. Comparison with the reference values of the Stanton number allows one to determine whether the current is laminar, turbulent or transient at a given point.

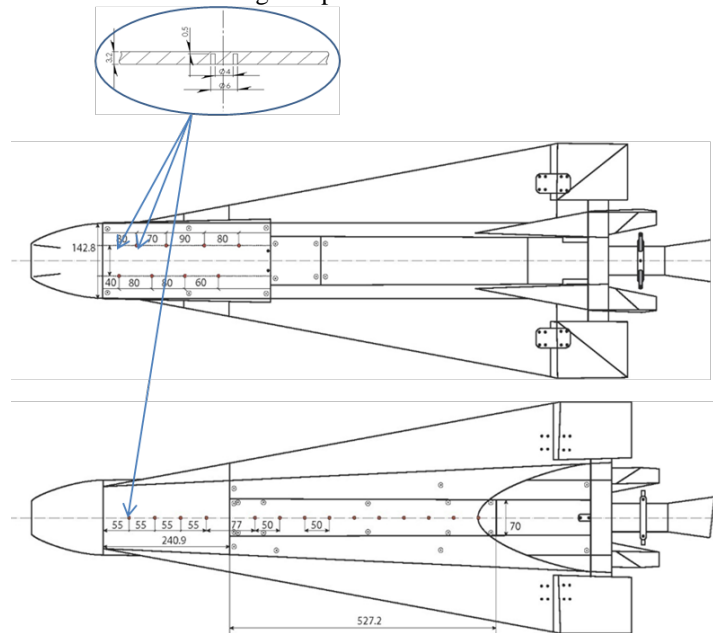


Figure 13: Location of thermocouples on leeward (top) and windward side (bottom).

4. Results comparison

The results of LTT studies obtained using various research methods: CFD, the experiment in the wind tunnel, and empirical formulas are summarized in Figures 14 and 15.

The above figures show the fields of the turbulence intensity parameter on the windward and leeward sides of the model, obtained using CFD methods (upper pictures in Figures 14 and 15). The graphs in the lower part of Figures 14 and 15 show the values of the Stanton number (St) in the plane of symmetry along the longitudinal coordinate. The black curves with the points correspond to the experimental data obtained in the TsAGI's wind tunnel T-116. Solid blue curves show the results of CFD modeling using the FLUENT package using the turbulence model with LT transition - Tran1. Solid green curves show the values of the St number obtained by TsAGI according to the empirical formulas (1), (2) and (3). The solid red curves show the values of the St number obtained by ESA according to their empirical formulas. The dotted blue and yellow curves show the results of the CFD simulation of the ESA using the TAU package with a fully turbulent PS (yellow point curves) and a fully simulations with laminar BL (blue dotted curves). The solid straight lines parallel to the vertical axis show the beginning of the LTT, obtained by ESA according to the Simeonides criterion for transition on the cone surface (blue line) and for transition on the flat plate surface (purple line). The method used to determine the origin and extent of LTT using the Simeonides criterion is described in detail in [8].

When assessing the consistency of results, one should take into account the complexity of the surface geometry and of the flow pattern around the model.

On the leeward side of the model, in both cases, all methods give values of the number St corresponding to the laminar BL. On the windward side, in the case of $M_\infty = 7$, $\alpha = 0^\circ$, different methods give the transition onset at a distance from the nose of 0.5 to 0.6 of the model length, then the transition zone extends to the end of the model. With an increase in the angle of attack on the windward side in the case of $M_\infty = 7$, $\alpha = 3.6^\circ$, the empirical ESA estimates and the TsAGI experiment give the transition onset at a distance of 0.6 to 0.7, while CFD simulation shows a later transition beginning after 0.8. However, in general, all the methods correctly reflect the fact that in the considered modes the flow around the EFTV HEXAFLY-INT model is transitional from laminar to turbulent.

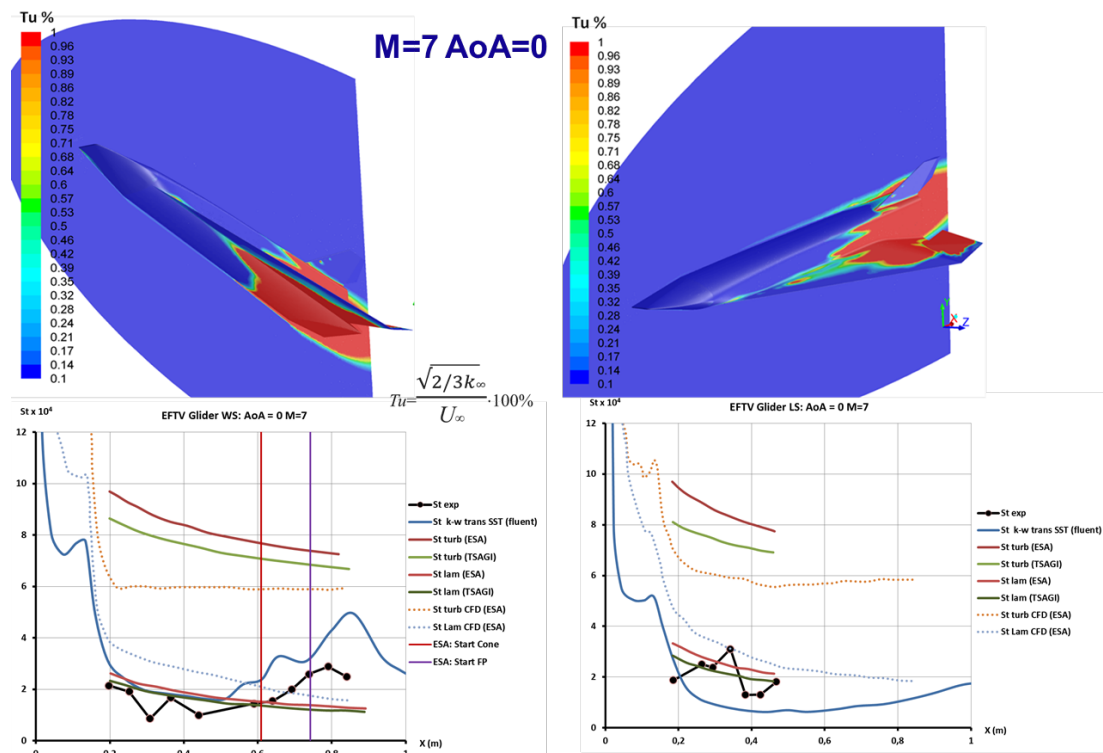


Figure 24: LTT results, obtained by different methods on windward (left) and leeward (right) sides; $M_\infty=7$, $\alpha=0^\circ$.

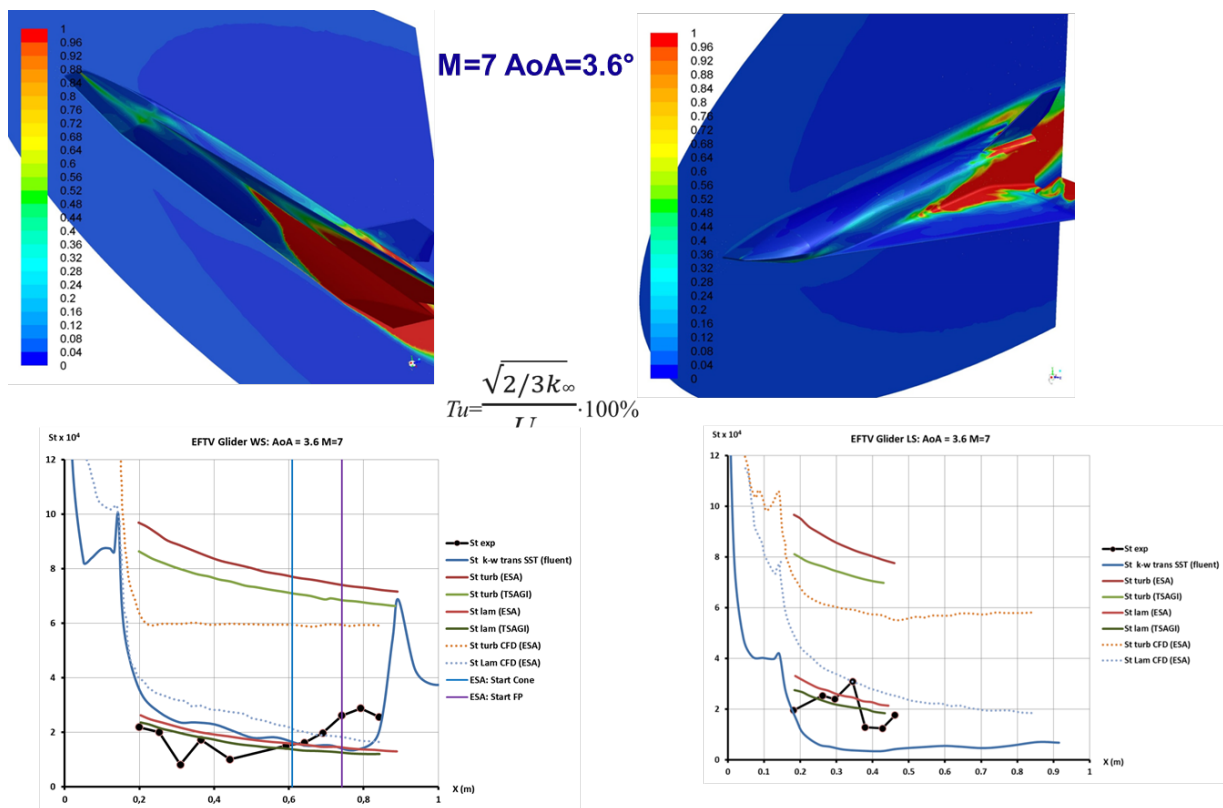


Figure 35: LTT results, obtained by different methods on windward (left) and leeward (right) sides; $M_\infty=7$, $\alpha=3.6^\circ$.

Conclusions

The present paper consider the laminar-to-turbulent transition for the EFTV glider at various regimes, corresponding to the points along the prospective flight trajectory. A variety of methods were deployed to simulate the LT transition.

Generally, the simulations for LTT seem to qualitatively agree with what is observed experimentally in the wind tunnel T-116 at TsAGI. On the windward side the transition onset starts for the various attitudes around midway whereas no clear transition is detected on the leeward side. The flow pattern on this leeward side is quite affected by three-dimensional vortical structures which render the heat loads higher than one would expect from turbulent correlations on a flat plate.

CFD simulations with two different LTT models Tran1 and Tran2 give significantly different flow patterns around EFTV. A comparison with experimental and empirical data makes it possible to conclude that the simulation with Tran1 is more adequate than with Tran2.

Acknowledgments

This work was performed within the ‘High-Speed Experimental Fly Vehicles-International’ project fostering International Cooperation on Civil High-Speed Air Transport Research. HEXAFly-INT, coordinated by ESA-ESTEC, is supported by the EU within the 7th Framework Programme Theme 7 Transport, Contract no.: ACP0-GA-2014-620327 and by the Ministry of Industry and Trade, Russian Federation. Further info on HEXAFly-INT can be found on <http://www.esa.int/hexafly-int>.

References

- [1] Steelant J., Langener T., Hannemann K., Riehmer J., Kuhn M., Dittert C., Jung W., Marini M., Pezzella G., Cicala M. and Serre L. 2015. Conceptual Design of the High-Speed Propelled Experimental Flight Test Vehicle

- HEXAFLY. In: *20th AIAA International Space Planes and Hypersonic Systems and Technologies Conference*, 5-8 July, Glasgow, Scotland, AIAA-2015-3539.
- [2] Favaloro N., Pezzella G., Carandente V., Scigliano R., Cicala M., Morani G. and Steelant J. 2015. Design Analysis of the High-Speed Experimental Flight Test Vehicle HEXAFLY-International. In: *20th Int. Space Planes and Hypersonic Systems and Technology Conference*, 5-8 July, Glasgow, Glasgow, Scotland, AIAA-2015-3607.
- [3] Steelant J., Marini M., Pezzella G., Reimann B., Chernyshev S.L., Gubanov A.A., Talyzin V.A., Voevodenko N.V., Kukshinov N.V., Prokhorov A.N., Neely A.J, Kennel C., Verstraete D., Buttswort D. 2016. Numerical and Experimental Research on Aerodynamics of High-Speed Passenger Vehicle within the HEXAFLY-INT Project. In: *30th Congress of the International Council of Aeronautical Sciences (ICAS)*, 25-30/09/2016, Daejeon, Korea.
- [4] Rini, P. 2006. Analysis of differential diffusion phenomena in high enthalpy flows, with application to thermal protection material testing in ICP facilities. PhD Thesis. Université Libre de Bruxelles, Faculté des Sciences Appliquées.
- [5] Kondratiev G.M. 1954. Regular heating regime. In: *Technical theoretical literature edition*.
- [6] Shvaley Yu. G. 1978. Experimental investigation of the local heat transfer in laminar boundary layer at supersonic velocities. *TsAGI scientific notes*. Vol. IX, № 5.
- [7] Ragulin N.F. and Shvaley Yu. G. 1983. Experimental investigation of the local heat transfer in turbulent boundary layer at supersonic velocities. *Journal of Engineering and Physics*. Vol. XLV, №4, 1983.
- [8] Steelant J., Passaro A., Fernandez-Villace V., Gubanov A., Ivanyushkin D., Shvaley Yu., Voevodenko N., Marini M., Benedetto S. 2017. Boundary Layer Transition Assessment on a Slender High-Speed Vehicle. In: *21th AIAA International Space Planes and Hypersonic Systems and Technologies Conference*, Xiamen, China, 6-9 March 2017: AIAA 2017-2316.